Nitrogen-doped graphene approach to enhance the performance of a membraneless enzymatic biofuel cell

Alireza Ahmadian Yazdi [a], Jie Xu [a, 1]

[a] *Department of Mechanical and Industrial Engineering, University of Illinois at Chicago, Chicago, IL 60607, USA*

Abstract

Heteroatom-doping of pristine graphene is an effective route for tailoring new characteristics in terms of catalytic performance which open up potentials for new applications in energy conversion and storage devices. Nitrogen-doped graphene (N-graphene), for instance, has shown excellent performance in many electrochemical systems involving oxygen reduction reaction (ORR), and more recently glucose oxidation. Owing to the excellent H_2O_2 sensitivity of N-graphene, the development of highly sensitive and fast-response enzymatic biosensors is made possible. However, a question that needs to be addressed is whether or not improving the anodic response to glucose detection may lead to a higher overall performance of enzymatic biofuel cell (eBFC). Thus, here we first synthesized N-graphene via a catalyst-free single-step thermal process, and made use of it as the biocatalyst support in a membraneless eBFC to identify its role in altering the performance characteristics. Our findings demonstrate that the electron accepting nitrogen sites in the graphene structure enhances the electron transfer efficiency between the mediator (redox polymer), redox active site of the enzymes, and electrode surface. Moreover, the best performance in terms of power output and current density of eBFCs was observed when the bioanode was modified with highly doped N-graphene.

Keywords: Enzymatic fuel cell, Nitrogen-doped graphene, Reduced graphene oxide, Catalyst-free synthesis

1. Introduction

Enzymatic biofuel cells (eBFCs) offer unique features in comparison to chemical fuel cells such as operation at room temperature and near neutral pH, ease of miniaturization, cheap organic fuels, small environmental footprint, *etc*. [1-3]. An eBFC operation is dependent upon the enzymatic biocatalysts that are often immobilized on the bioanode and biocathode. On the bioanode side enzymes such as glucose oxidase (GOx) catalyze the oxidation of biofuels such as glucose [4, 5], fructose [6, 7], or alcohols [8], while an oxidant, *e.g.* oxygen (O_2), is reduced enzymatically at the biocathode. In glucose eBFCs the overall cell reaction is the consumption of glucose and oxygen and the production of gluconolactone as well as hydrogen peroxide and water. Depending on the application, many configurations of eBFCs have been proposed over the years, which can be categorized mainly as either with or without membrane. In general, in membrane-containing cells the bioanode and biocathode are separated by a polymeric layer preferably closer to the cathodic side. The role of membrane is often attributed to

[1] Corresponding author:
E-mail address: jiexu@uic.edu (J. Xu)

the regulation of ions between the bioanodes and biocathodes, and preventing the diffusion of reaction byproducts from reaching the opposite side of the cell. However, this is often accompanied with higher internal ohmic resistance and power loss, and many attempts have been made to safely remove the membrane while maintaining cell stability and enzymatic activity for long operating cycles.

Graphene and its derivatives possess unique features such as high surface area, good electronic conductivity, ease of synthesis and functionalization, that enable their use for biosensing as well as energy-related applications. Over the years, researchers have recognized chemical functionalization of graphene structures as an effective tool to tailor new features, especially catalytic performance towards oxygen reduction reaction (ORR) [9], hydrogen evolution reaction (HER) [10], and oxygen evolution reaction (OER) [11]. These reactions are of huge importance for the state-of-the-art battery and fuel cell design, as well as electrosynthesis of biofuels. Generally, heteroatom-doped graphene such as boron and nitrogen-doped graphene (N-graphene), exhibits different properties than pristine graphene in terms of charge distribution of carbon atoms, leading to activated regions with catalytic performance on the graphene structure [12]. Wang et al. [13], were among the first group to investigate the role of N-graphene on glucose sensitivity in a typical GOx-based biosensor. Their study has shown that nitrogen sites in the graphene structure drastically enhance amperometric response in glucose monitoring. These results open up great potentials for developing next generation amperometric glucose biosensors with high sensitivity and fast response.

In an eBFC, often the cathodic reaction is the rate limiting step, meaning that enhancing the overall cell performance by improving anodic reaction or glucose sensitivity is only a possibility. Thus, in this study, we turned our attention to the impact of N-graphene as the support material for bioanode on the overall eBFC performance. First of all, N-graphene was synthesized via a thermal reduction of graphite oxide (GO) in the presence of melamine as the nitrogen precursor. Next, carbon paper substrates were modified with N-graphene graphene and reduced graphene oxide (rGO), and their electrochemical communication with GOx/redox polymer hydrogel as the biocatalyst was studied. Finally, in conjunction with a bilirubin oxidase (BOx) biocathode, we fabricated a membraneless eBFCs to reveal the impact of N-graphene on the cell overall performance.

2. Experimental

2.1. Materials and chemicals

Glucose oxidase (GOx, from *'Aspergillus niger'*, EC 1.1.3.4, Type X-S), tetrabutylammonium bromide (TBAB), (6-Bromohexyl) ferrocene, and melamine were purchased from Sigma-Aldrich. Citric acid, sodium phosphate dibasic anhydrous, and dextrose (D-glucose) anhydrous were purchased from Fisher Scientific. LPEI (MW 100,000) and ethylene glycol diglycidyl ether (EGDGE) were ordered from Polyscience Inc., Warrington, PA. Bilirubin oxidase (BOx from *'Myrothecium sp.'*, EC 1.3.3.5) was purchased from Amano Enzyme Inc. Carbon paper MGL280 (non-wet proofed) was purchased from Fuel Cell Earth. Graphite oxide, produced by modified Hummer's method, was obtained from ACS Material. All chemicals were used as received without further purification.

TBAB-modified Nafion was synthesized following the reported procedure in [14, 15]. Anthracene-modified multi-walled carbon nanotubes (An-MWCNTs) were modified as described in [16-18]. The electron transfer in the bioanode is mediated by hexylferrocenyl-LPEI (Fc-C_6-LPEI) redox polymer. The synthesis of Fc-C_6-LPEI has been described in [19, 20]. In short, 300 mg of linear polyethylenimine were added to 10 mL of acetonitrile. The solution was then heated to reflux for approximately 10 minutes. Next, 380 mg of (6-Bromohexyl)ferrocene in 2 mL of ethanol were added to the mixture and heated to reflux solvent for about 12 hours. Afterwards, the polymer was extracted under reduced pressure, and the remaining residues were rinsed by diethyl ether which helps to remove the ferrocenyl impurities.

2.2. Instrumentation

CHI 660E potentiostat (CH Instrument, USA) was utilized for electrochemical analysis. Electrocatalysis investigation of bioelectrodes was conducted in a standard three-electrode setup where a saturated calomel electrode (SCE) and a platinum mesh (1 cm^2 projected surface area) were used as reference and counter electrodes, respectively. All the electrochemical tests were performed in a 0.2 M citrate/phosphate buffer solution (pH 7.0) as the supporting electrolyte, and at room temperature (21 ℃). Current and power densities were normalized with respect to the projected surface area of the anode. Raman spectroscopy was carried out using Renishaw inVia Reflex Raman, with a 532 nm wavelength laser.

2.3. Bioelectrode fabrication

The bioelectrodes were fabricated following the procedures reported in [21, 22]. To prepare 3 cm^2 of BOx/An-MWCNT/TBAB-modified Nafion cathodes, 1.5 mg of BOx was dissolved in 75 µL of 0.2 M citrate/phosphate buffer (pH 7.0). Next, 7.5 mg of An-MWCNTs were added to the solution and vortex mixed for 1 minute, followed by sonication for 15 seconds. This step was repeated three times to obtain a homogenized enzymatic paste. Then, 25 µL of TBAB-modified Nafion was added to the mixture, followed by three steps of vortex mixing and sonication. The resulting paste was then coated on the carbon paper electrodes using a brush, and dried at room temperature under positive air flow for about 4 hours. Fabrication of 6 $cm^2$of GOx/Fc-C_6-LPEI bioanode starts with preparing an enzymatic redox hydrogel. Briefly, 210 µL of 10 mg mL^{-1} hexylferrocenyl-LPEI polymer in DI water was mixed with 90 µL of 10 mg mL^{-1} GOx solution in DI water. Then, 11.25 µL of EGDGE solution (10% v/v in DI water) was added to the mixture, and vortex mixed for about 30 seconds. The hydrogel was then pipetted on carbon paper electrodes, and left at room temperature for 24 hours to dry. Before coating with hydrogel, the carbon paper substrates were modified with 100 µL of 10 mg mL^{-1} (in ethanol) rGO or functionalized graphene solution. This procedure involves drop casting the solution on to the substrate, and drying it at room temperature for 12 hours.

2.4. Synthesis of N-graphene

Nitrogen doped graphene was synthesized via a simple one-step thermal annealing of GO in the presence of various amounts of melamine acting as the nitrogen doping precursor [23, 24]. Briefly, GO and melamine (1:5 and 1:50 ratios) were ground together with a pestle in a mortar for about 5 minutes. Afterwards, the mixture was loaded to a crucible with lid and placed in the center of a chemical vapor deposition furnace (CVD). Initially, the

furnace was purged with argon gas for 1 hour to ensure the removal of O_2 in the reaction tube. Then, the temperature was raised at a rate of 5 ℃ min^{-1}, and maintained at 900 ℃ for 30 minutes. Finally the furnace was slowly cooled down to the room temperature under argon atmosphere. To synthesize reduced graphene oxide (rGO), the above steps were repeated without the addition of melamine.

3. Results and discussion

3.1. Graphene functionalization

Raman spectroscopy is recognized as a non-destructive technique for characterizing carbon materials [25]. The Raman spectra of the GO, as-synthesized rGO and N-graphene were obtained, and the peak position and intensities were analyzed. As shown in Fig. 1, the Raman spectra demonstrate noticeable peaks at *ca.* 1580 and 1350 cm^{-1} corresponding to G and D band, respectively. Sheng et al. [24] have shown that increasing the melamine content in the precursor from 1:5 to 1:50 increases the N-doping level from *ca.* 6.6% to 8.4% at the same synthesis temperature of 800 ℃. Higher doping level is often accompanied by more defects such as holes and generation of edges in the graphene structure, leading to an enhanced relative intensity of the D band [23, 26]. This is consistent with the results observed in Fig. 1, where the I_D/I_G is increasing as the doping level increases. Moreover, analyzing the peak position of G band demonstrates a downshift from *ca.* 1586 cm^{-1} for GO to 1584 and 1583 cm^{-1} for N-graphene (1:5) and (1:50), respectively. This downshift of G position has been recognized as a sign for successful N-doping of graphene structure [23, 27].

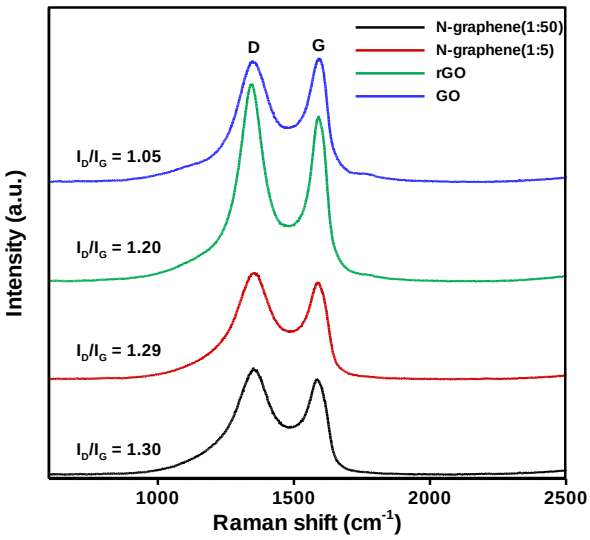

Fig. 1. Raman spectra of GO, rGO, and N-graphene with different mass ratio of GO to melamine during the synthesis.

3.2. The role of N-graphene on eBFC performance

The typical mechanism of glucose oxidation by GOx enzymes is as follows [21]:

$$\mathrm{GOx(FAD) + Glucose \rightarrow GOx(FADH_2) + Gluconolactone} \quad (1)$$

$$\mathrm{GOx(FADH_2) + O_2 \rightarrow GOx(FAD) + H_2O_2} \quad (2)$$

where flavin adenine dinucleotide (FAD) acts as the redox co-factor of GOx. In this reaction scheme, parasitic H_2O_2 results from an incomplete oxidation of glucose, and is a common byproduct of catalysis by oxidase enzymes. The accumulation of H_2O_2 can negatively affect the enzymatic activity and stability of the electrode especially in long operating cycles. One approach to alleviate this problem is the introduction of H_2O_2 reducing agents to the bioelectrodes. Prussian blue, for instance, can catalyze the reduction of H_2O_2, and has been incorporated into the enzymatic bioanodes for enhancing glucose sensitivity in biosensing applications [28-30]. Regarding eBFCs, the H_2O_2 reducing agents may be combined with cathodic catalyst to protect the cathodic environment from peroxide contamination or deactivation of the cathodic enzymes, especially in a membraneless configuration. For instance, our group recently introduced a novel membraneless biobattery by using a Prussian blue modified cathode that can act both as a rechargeable material and reductant of the H_2O_2 diffused from the bioanode [31]. N-graphene can also dramatically increase the H_2O_2 electrocatalyis, and thus enhance the biosensing ability of GOx-based electrodes in terms of glucose detection [13]. However, as mentioned earlier, the rate limiting step in the overall eBFC reaction is the cathodic reaction, meaning that the bioanode improvement may have less impact on the overall performance which is addressed in the remaining sections.

3.3. Enzymatic biocatalytic performance

At first, we investigated the electrocatalysis of enzymatic bioanodes towards oxidizing glucose by modifying them with rGO and N-graphene with two different doping levels of nitrogen atoms. As shown in Fig. 2a, the catalytic current dramatically increases, and the onset potential slightly decreases by incorporating rGO and N-graphene as the support material for GOx immobilization. This is mainly attributed to the higher peroxide sensitivity of graphene doped bioanodes [13]. Moreover, heteroatom-doped graphene offers superior electronic conductivity which may enhance the communication between the active sites of the enzyme, mediator, and electrode surface. To investigate this phenomenon, cyclic voltammetry in the absence of glucose was applied to the N-graphene modified electrode with high nitrogen content and the results were compared against bare carbon paper substrate (blank). As illustrated in Fig. 2b, the redox pair in both cases may correspond to the redox reaction of Fc-C_6-LPEI between the active site of the GOx and the electrode surface. Clearly, applying N-graphene increases the rate of this reaction, signifying a superior electron transfer efficiency.

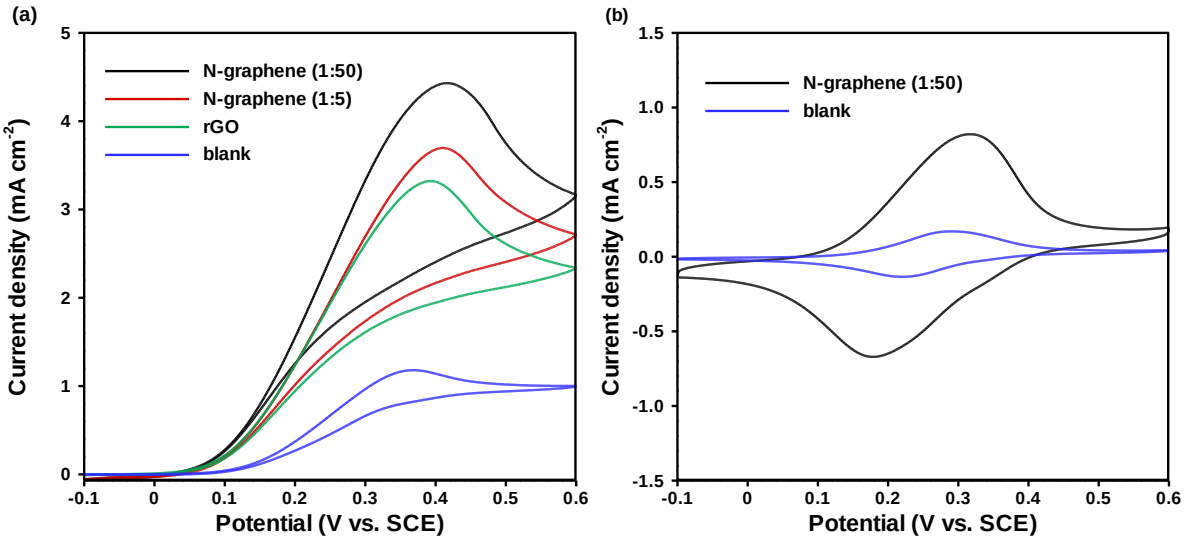

Fig. 2. Representative cyclic voltammograms of the as-prepared GOx/Fc-C_6-LPEI bioanodes (a) modified with rGO and N-graphene in the presence of 0.1 M glucose, and (b) modified with N-graphene (1:50) and bare carbon paper (blank) in the absence of glucose, at a scan rate of 10 mV s^{-1}.

In the next section we investigated the overall performance of eBFC by combining the modified bioanodes with a BOx/An-MWCNT/TBAB-modified Nafion biocathode. However, before proceeding, the fabricated biocathodes were studied using cyclic voltammetry to ensure the immobilization of the BOx enzymes and their proper biocatalytic performance. As shown in Fig. 3, the addition of O_2 to the electrolyte significantly enhances the cathodic current which is a signal for ORR being catalyzed by BOx enzymes.

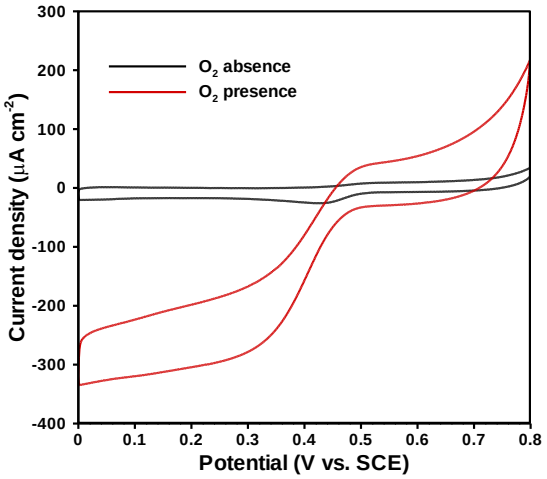

Fig. 3. Representative cyclic voltammograms of the as-prepared BOx/An-MWCNT/TBAB-modified Nafion biocathode in the absence and presence of O_2, at a scan rate of 10 mV s^{-1}.

3.4. eBFC performance

The eBFC studied here is within a membraneless configuration, since we anticipate the majority of H_2O_2 forming at the bioanode is reduced by N-graphene, enabling less peroxide crossover to the biocathode. Moreover, removing the membrane lowers the internal ohmic resistance, leading to a more efficient performance. Fig. 4 demonstrates the power output of the eBFC with the corresponding modified bioanodes. These power curves were obtained by sweeping the voltage between the open circuit voltage (OCV) of the cell to 0 at a scan rate of 1 mV s^{-1}. Before the linear polarization tests, the OCV of the eBFC setup was measured by maintaining the cell at zero current until a stable voltage over time is observed. Prior to the performance tests, the electrolyte was injected with O_2 for half an hour to ensure the presence of enough oxidant for cathodic reaction (O_2-reducing BOx).

As evident by the results in Fig. 4, the eBFCs modified with N-graphene demonstrate higher maximum power output and current density compared to the rGO and plain carbon paper (blank). Moreover, increasing the N-content of graphene structure further enhances the power output, illustrating the role of electron accepting nitrogen atoms in improving the performance characteristics. The reaction scheme (1) and (2), suggests that as we increase the O_2 content of the electrolyte comparably more H_2O_2 will be produced by GOx enzymes. Our experimental setup mimics this condition where bioelectrodes are placed in the O_2 saturated environment. On the other hand, as mentioned earlier, N-graphene exhibits superior H_2O_2 sensitivity over graphene [13]. Thus, we may conclude that the majority of the power increase by N-doping of graphene stems from its electron accepting properties and catalytic performance towards reducing H_2O_2.

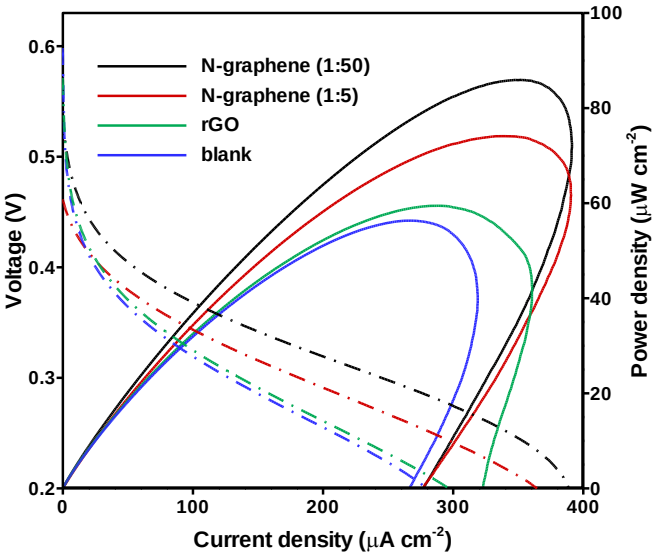

Fig. 4. Power curves (solid lines) and linear polarization graphs (dashed lines) of the eBFCs equipped with GOx/Fc-C_6-LPEI bioanodes modified with N-graphene (1:5) and (1:50), rGO, and bare carbon paper (blank).

Table 1 summarizes the results by comparing the performance of N-graphene modified eBFCs versus rGO and unmodified case (blank). As seen, N-graphene is a superior choice over rGO and bare carbon paper for biocatalyst support, mainly due to higher H_2O_2 sensitivity and better electron transfer efficiency between enzyme, redox mediator, and electrode surface. Moreover, N-graphene (1:50) corresponding to a higher level of nitrogen doping,

exhibits the maximum increase in power (by *ca.* 41%) and current density, illustrating the role of electron accepting nitrogen sites in enhancing eBFC's power output.

Table 1. Comparison of eBFCs performance with different bioanode modifications.

Anode modification	OCV (~V)	Maximum power density (~μW cm^{-2})	Current density at maximum power (~μA cm^{-2})	Power increase *vs.* blank (~%)
N-graphene (1:50)	0.55	85.91	355.00	41
N-graphene (1:5)	0.55	74.09	339.90	35
rGO	0.56	59.45	288.60	14
blank	0.56	55.97	252.10	-

4. Conclusion

In this work, our aim was to identify the role of heteroatom-doped graphene and the mechanisms by which it may impact the eBFC overall performance. As a proof-of-concept, N-graphene widely used as ORR catalyst in batteries and fuel cells was chosen, and its impact was investigated on eBFC's operation with a membraneless design. The results of the present work are of high practical importance for the design and optimization of self-powered biosensors, eBFCs, and implantable enzymatic devices. For instance, the peroxide formation in implantable devices may hinder the application of conventional eBFCs, as the peroxide might be toxic both towards the enzymatic bioelectrodes and living tissue cells. Additionally, peroxide accumulation diminishes the life time of both cathodic and anodic enzymes, leading to destabilized performance. By incorporating the H_2O_2 reducing agent in the eBFC design we may alleviate some of these issues, and ensure a safer operation of membraneless configurations.

Acknowledgement

We highly thank Dr. Shelley D. Minteer, Dr. Ross D. Milton, and Dr. David P. Hickey at the University of Utah for kindly providing us with An-MWCNT and for their guidelines and support. This work also made use of instruments in the Electron Microscopy Service (EMS), at the Research Resources Center, University of Illinois at Chicago.

References

1. Rasmussen, M., S. Abdellaoui, and S.D. Minteer, *Enzymatic biofuel cells: 30 years of critical advancements.* Biosensors and Bioelectronics, 2016. **76**: p. 91-102.
2. Meredith, M.T. and S.D. Minteer, *Biofuel cells: enhanced enzymatic bioelectrocatalysis.* Annual Review of Analytical Chemistry, 2012. **5**: p. 157-179.
3. Yazdi, A.A., et al., *Carbon nanotube modification of microbial fuel cell electrodes.* Biosensors and Bioelectronics, 2016. **85**: p. 536-552.
4. Pankratov, D., et al., *Transparent and flexible, nanostructured and mediatorless glucose/oxygen enzymatic fuel cells.* Journal of Power Sources, 2015. **294**: p. 501-506.
5. Milton, R.D., et al., *Employing FAD-dependent glucose dehydrogenase within a glucose/oxygen enzymatic fuel cell operating in human serum.* Bioelectrochemistry, 2015. **106**: p. 56-63.

6. Zhang, L., et al., *Towards High-Voltage Aqueous Metal-Ion Batteries Beyond 1.5 V: The Zinc/Zinc Hexacyanoferrate System.* Advanced Energy Materials, 2015. **5**(2).
7. Ogawa, Y., et al., *Stretchable biofuel cell with enzyme-modified conductive textiles.* Biosensors and Bioelectronics, 2015. **74**: p. 947-952.
8. Aquino Neto, S., et al., *Membraneless enzymatic ethanol/O2 fuel cell: Transitioning from an air-breathing Pt-based cathode to a bilirubin oxidase-based biocathode.* Journal of Power Sources, 2016. **324**: p. 208-214.
9. Qu, L., et al., *Nitrogen-doped graphene as efficient metal-free electrocatalyst for oxygen reduction in fuel cells.* ACS nano, 2010. **4**(3): p. 1321-1326.
10. Ito, Y., et al., *High Catalytic Activity of Nitrogen and Sulfur Co-Doped Nanoporous Graphene in the Hydrogen Evolution Reaction.* Angewandte Chemie International Edition, 2015. **54**(7): p. 2131-2136.
11. Lin, Z., et al., *Simple preparation of nanoporous few-layer nitrogen-doped graphene for use as an efficient electrocatalyst for oxygen reduction and oxygen evolution reactions.* Carbon, 2013. **53**: p. 130-136.
12. Wang, H., T. Maiyalagan, and X. Wang, *Review on recent progress in nitrogen-doped graphene: synthesis, characterization, and its potential applications.* Acs Catalysis, 2012. **2**(5): p. 781-794.
13. Wang, Y., et al., *Nitrogen-doped graphene and its application in electrochemical biosensing.* ACS nano, 2010. **4**(4): p. 1790-1798.
14. Thomas, T.J., et al., *Effects of annealing on mixture-cast membranes of Nafion® and quaternary ammonium bromide salts.* Journal of membrane science, 2003. **213**(1): p. 55-66.
15. Akers, N.L., C.M. Moore, and S.D. Minteer, *Development of alcohol/O 2 biofuel cells using salt-extracted tetrabutylammonium bromide/Nafion membranes to immobilize dehydrogenase enzymes.* Electrochimica Acta, 2005. **50**(12): p. 2521-2525.
16. Dawn, A., et al., *Transcription of chirality in the organogel systems dictates the enantiodifferentiating photodimerization of substituted anthracene.* Chemistry–A European Journal, 2010. **16**(12): p. 3676-3689.
17. Minson, M., et al., *High performance glucose/O2 biofuel cell: Effect of utilizing purified laccase with anthracene-modified multi-walled carbon nanotubes.* Journal of The Electrochemical Society, 2012. **159**(12): p. G166-G170.
18. Milton, R.D., et al., *Bilirubin oxidase bioelectrocatalytic cathodes: the impact of hydrogen peroxide.* Chemical Communications, 2014. **50**(1): p. 94-96.
19. Merchant, S.A., et al., *High-sensitivity amperometric biosensors based on ferrocene-modified linear poly (ethylenimine).* Langmuir, 2009. **25**(13): p. 7736-7742.
20. Merchant, S.A., et al., *Effect of mediator spacing on electrochemical and enzymatic response of ferrocene redox polymers.* The Journal of Physical Chemistry C, 2010. **114**(26): p. 11627-11634.
21. Milton, R.D., et al., *Hydrogen peroxide produced by glucose oxidase affects the performance of laccase cathodes in glucose/oxygen fuel cells: FAD-dependent glucose dehydrogenase as a replacement.* Physical Chemistry Chemical Physics, 2013. **15**(44): p. 19371-19379.
22. Meredith, M.T., et al., *High current density ferrocene-modified linear poly (ethylenimine) bioanodes and their use in biofuel cells.* Journal of the Electrochemical Society, 2011. **158**(2): p. B166-B174.
23. Lin, Z., et al., *Facile preparation of nitrogen-doped graphene as a metal-free catalyst for oxygen reduction reaction.* Physical Chemistry Chemical Physics, 2012. **14**(10): p. 3381-3387.

24. Sheng, Z.-H., et al., *Catalyst-free synthesis of nitrogen-doped graphene via thermal annealing graphite oxide with melamine and its excellent electrocatalysis.* ACS nano, 2011. **5**(6): p. 4350-4358.
25. Das, A., et al., *Monitoring dopants by Raman scattering in an electrochemically top-gated graphene transistor.* Nature nanotechnology, 2008. **3**(4): p. 210-215.
26. Jia, Y., et al., *Defect graphene as a trifunctional catalyst for electrochemical reactions.* Advanced Materials, 2016. **28**(43): p. 9532-9538.
27. Wei, D., et al., *Synthesis of N-doped graphene by chemical vapor deposition and its electrical properties.* Nano letters, 2009. **9**(5): p. 1752-1758.
28. Karyakin, A.A., *Prussian blue and its analogues: electrochemistry and analytical applications.* Electroanalysis, 2001. **13**(10): p. 813-819.
29. Zhao, W., et al., *Multilayer membranes via layer-by-layer deposition of organic polymer protected Prussian blue nanoparticles and glucose oxidase for glucose biosensing.* Langmuir, 2005. **21**(21): p. 9630-9634.
30. Karyakin, A.A., O.V. Gitelmacher, and E.E. Karyakina, *Prussian blue-based first-generation biosensor. A sensitive amperometric electrode for glucose.* Analytical chemistry, 1995. **67**(14): p. 2419-2423.
31. Yazdi, A.A., et al., *Rechargeable membraneless glucose biobattery: Towards solid-state cathodes for implantable enzymatic devices.* Journal of Power Sources, 2017. **343**: p. 103-108.